nature biotechnology

Rescue of the spinal muscular atrophy phenotype in a mouse model by early postnatal delivery of *SMN*

Kevin D Foust[1], Xueyong Wang[2,6], Vicki L McGovern[3,6], Lyndsey Braun[1], Adam K Bevan[1,4], Amanda J Haidet[1,4], Thanh T Le[3], Pablo R Morales[5], Mark M Rich[2], Arthur H M Burghes[3,4] & Brian K Kaspar[1,4]

Spinal muscular atrophy (SMA), the most common autosomal recessive neurodegenerative disease affecting children, results in impaired motor neuron function[1]. Despite knowledge of the pathogenic role of decreased survival motor neuron (SMN) protein levels, efforts to increase SMN have not resulted in a treatment for patients. We recently demonstrated that self-complementary adeno-associated virus 9 (scAAV9) can infect ~60% of motor neurons when injected intravenously into neonatal mice[2–4]. Here we use scAAV9-mediated postnatal day 1 vascular gene delivery to replace *SMN* in SMA pups and rescue motor function, neuromuscular physiology and life span. Treatment on postnatal day 5 results in partial correction, whereas postnatal day 10 treatment has little effect, suggesting a developmental period in which scAAV9 therapy has maximal benefit. Notably, we also show extensive scAAV9-mediated motor neuron transduction after injection into a newborn cynomolgus macaque. This demonstration that scAAV9 traverses the blood-brain barrier in a nonhuman primate emphasizes the clinical potential of scAAV9 gene therapy for SMA.

Proximal SMA results in motor neuron death in the spinal cord. SMA is caused by loss of survival motor neuron gene 1 (*SMN1*) and retention of *SMN2*, resulting in reduced levels of SMN, a ubiquitously expressed protein important in the assembly of ribonucleoprotein complexes[1,5–7]. Neuronal expression of SMN appears essential[8]. Recent work using a double transgenic knockout mouse model of SMA showed that postnatal lentiviral-mediated delivery of SMN to motor neurons increased survival by 3–5 d in an animal that normally survives ~13 d[9]. Pharmacological approaches have increased survival up to ~40 d[10,11]. We and others recently demonstrated that intravenous injection of scAAV9 into 1-d-old (postnatal day 1, P1) mice and cats infects ~60% of motor neurons, indicating the potential of this approach in treating SMA[2,12]. Here, we report that scAAV9-mediated *SMN* gene replacement (with scAAV9-SMN) in SMA mice results in an unprecedented improvement in survival and motor function[13]. We also show that scAAV9–green fluorescent protein (GFP) crosses the blood-brain barrier in a nonhuman primate and transduces motor neurons, supporting the possibility of translating this treatment option to human patients.

To determine transduction levels in SMA mice (*SMN2*$^{+/+}$; *SMN*Δ*7*$^{+/+}$; *Smn*$^{-/-}$), we injected 5×10^{11} genomes of scAAV9-GFP or scAAV9-SMN (n = 4/group) under control of the chicken-β-actin hybrid promoter into the facial vein on P1. We found that 42 ± 2% of lumbar spinal motor neurons expressed GFP (**Fig. 1a** and **Supplementary Table 1**) 10 d after injection. The levels of SMN in the brain, spinal cord and muscle in scAAV9-SMN–treated animals are shown in **Figure 1b**. SMN levels were increased in brain, spinal cord and muscle in treated animals, but were still lower than controls (*SMN2*$^{+/+}$; SMNΔ7$^{+/+}$; *Smn*$^{+/-}$) in neural tissue (**Supplementary Fig. 1**). Spinal cord immunohistochemistry demonstrated expression of SMN within choline acetyl transferase (ChAT)-positive cells after scAAV9-SMN injection (**Supplementary Fig. 2**).

We next evaluated whether scAAV9-SMN treatment of SMA animals improved motor function[14]. SMA animals treated with scAAV9-SMN or scAAV9-GFP on P1 were assessed for the ability to right themselves compared to control and untreated animals (n = 10/group). Control animals could right themselves quickly, whereas the SMN- and GFP-treated SMA animals showed difficulty at P5. However, by P13, 90% of SMN-treated animals could right themselves compared with 20% of GFP-treated controls and 0% of untreated SMA animals, suggesting that SMN-treated animals improved (**Fig. 1c**). At P18, SMN-treated animals were larger than GFP-treated animals but smaller than controls (**Fig. 1d**). Locomotive ability of the SMN-treated animals was nearly identical to that of controls as assayed by x, y and z plane beam breaks (open field testing) and wheel running (**Supplementary Figs. 3** and **4** and **Supplementary Movie**). Age-matched untreated SMA animals were not available as controls for open field or running wheel analysis owing to their short life span.

We next examined survival of SMN-treated SMA animals (n = 11) compared with GFP-treated SMA animals (n = 11). No GFP-treated control animals survived past P22, with a median life span of 15.5 d (**Fig. 1e**). We analyzed body weight in SMN- or GFP-treated animals compared to wild-type littermates. The GFP-treated animals' weights peaked at P10 and then precipitously declined until death. In contrast, SMN-treated animals showed a steady weight gain to approximately P40, where the weight stabilized at 17 g, half the weight of controls (**Fig. 1f**). The smaller size of corrected animals is likely related to

[1]Center for Gene Therapy, The Research Institute at Nationwide Children's Hospital, Columbus, Ohio, USA. [2]Wright State University, Dayton, Ohio, USA. [3]Department of Molecular and Cellular Biochemistry and [4]Integrated Biomedical Graduate Program, The Ohio State University, Columbus, Ohio, USA. [5]The Mannheimer Foundation, Inc., Homestead, Florida, USA. [6]These authors contributed equally to this work. Correspondence should be addressed to B.K.K. (Brian.Kaspar@NationwideChildrens.org).

Received 29 July 2009; accepted 28 January 2010; published online 28 February 2010; doi:10.1038/nbt.1610

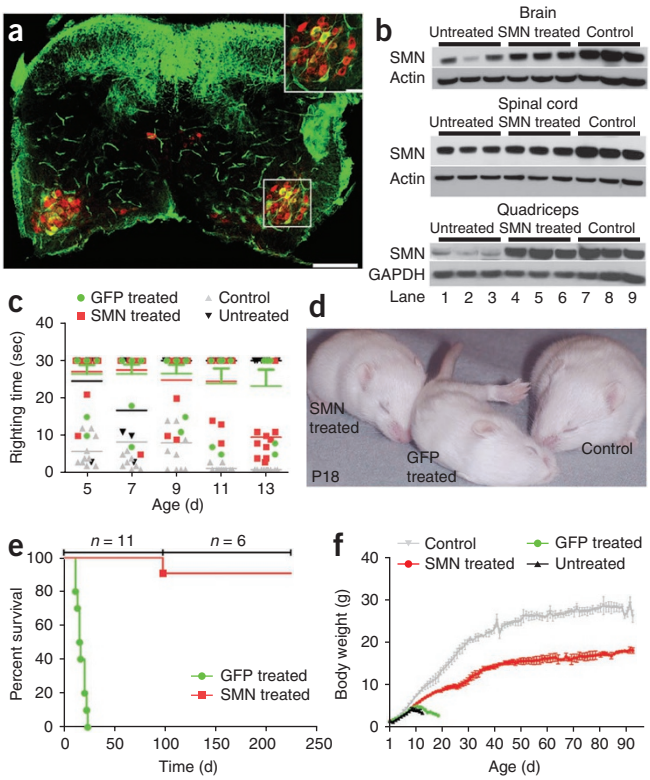

Figure 1 Phenotypic correction of SMA mice injected on P1. (**a**) Injection of scAAV9-GFP in SMA animals results in GFP expression (green) within dorsal root ganglia and motor neurons (ChAT staining in red) in the lumbar spinal cord 10-d post-injection. (**b**) Western blots from tissues of control, scAAV9-SMN–treated and untreated SMA animals show elevated levels of SMN expression in SMN-treated animals compared to control animals, although levels are still lower than those of control littermates. Quantifications of western blots are available in the **Supplementary Figures 1** and **7**. (**c**) Righting ability shows that SMN-treated animals can right themselves similarly to control animals by P13. (**d**) SMA animals treated with scAAV9-SMN are larger than GFP-treated animals. (**e**) scAAV9-SMN treatment of SMA animals results in greatly extended survival over GFP treatment. (**f**) Body weight assessments show increase in animals treated with scAAV9-SMN versus those treated with GFP. Scale bars, 200 μm (**a**); 50 μm (**a** inset).

the tropism and incomplete transduction of scAAV9, resulting in a 'chimeric' animal in which some cells are not transduced. Additionally, the smaller size suggests an embryonic role for SMN. Notably, no deaths occurred in the SMN-treated group until P97. Furthermore, this death appeared to be unrelated to SMA as the mouse died after trimming of long extensor teeth. We euthanized our animals (P90–99) for electrophysiology of neuromuscular junctions (NMJs). The remaining six animals were still alive as of resubmission in November 2009 and had surpassed 250 d of age.

A recent report demonstrated that neuromuscular transmission is abnormal in SMA mice[15]. To determine whether the reduction in endplate currents (EPCs) was corrected with scAAV9-SMN, we recorded EPCs from the tibialis anterior (TA) muscle. P9–P10 animals were evaluated to ensure the presence of the reported abnormalities. Control mice had an EPC amplitude of 19.1 ± 0.8 nA versus 6.4 ± 0.8 nA in untreated SMA animals (P = [illegible]), confirming published results[15]. Notably, scAAV9-SMN–treated SMA animals had a significant improvement at P10 over age-matched untreated SMA animals (8.8 ± 0.8 versus 6.4 ± 0.8 nA, $P < 0.$[illegible]). However, gene therapy treatment had not restored normal EPC at P10 when comparing scAAV9-SMN–treated SMA animals with controls (19.1 ± 0.8 versus 8.8 ± 0.8 nA, $P = 0.$[illegible]). At P90–P99, there was no difference in EPC amplitude between controls and SMA mice that had been treated with scAAV-SMN (**Fig. 2a**). Thus, treatment with scAAV9-SMN fully corrected the reduction in synaptic current. P90–P99 age-matched untreated SMA animals were not available as controls owing to their short life span.

The amplitude of EPCs is determined by the number of synaptic vesicles released after nerve stimulation (quantal content) and the amplitude of the muscle response to the transmitter released from a single vesicle (quantal amplitude). Untreated SMA mice have a reduction in EPC primarily because of reduced quantal content[15]. In our P9–P10 colony, untreated SMA animals had a reduced quantal content compared with wild-type controls (5.7 ± 0.6 versus 12.8 ± 0.6, $P < 0.05$), but scAAV9-SMN–treated animals were again improved over the untreated animals (9.5 ± 0.6 versus 5.7 ± 0.6, $P < 0.05$), but not to the level of wild-type animals (9.5 ± 0.6 versus 12.8 ± 0.6, $P < 0.05$). At P90–P99, the quantal content in treated SMA mice was

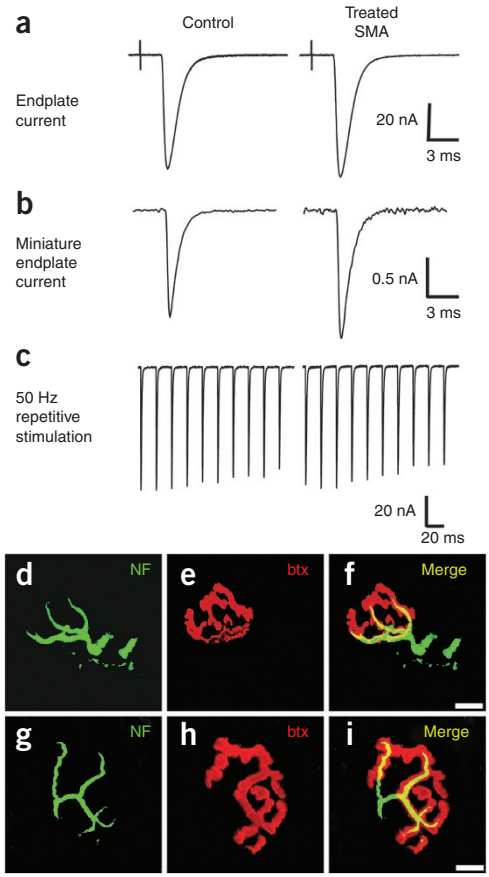

Figure 2 Effects of SMN treatment at P1 on NMJs of adult SMA mice. Untreated SMA mice do not survive to adulthood. (**a**) scAAV9-SMN treatment restores endplate currents (EPC) in ~90-d-old SMA animals. In control mice, the mean EPC amplitude was 82.6 ± 3.5 nA, and in treated SMA mice, it was 83.4 ± 4.1 nA ($P = 0.89$, $n = 4$ mice for each group). (**b**) Affected animals treated with scAAV9-SMN had an increase in miniature endplate currents. (**c**) Both control and treated SMA endplate currents had a similar degree of depression during 50 Hz nerve stimulation. (**d**–**i**) Representative sections from the transverse abdominis (TVA), a proximal muscle with innervation abnormalities in SMA mice[2], shows normal innervation in both wild-type (**d**–**f**) and SMN-treated (**g**–**i**) animals. Scale bars, 10 μm.

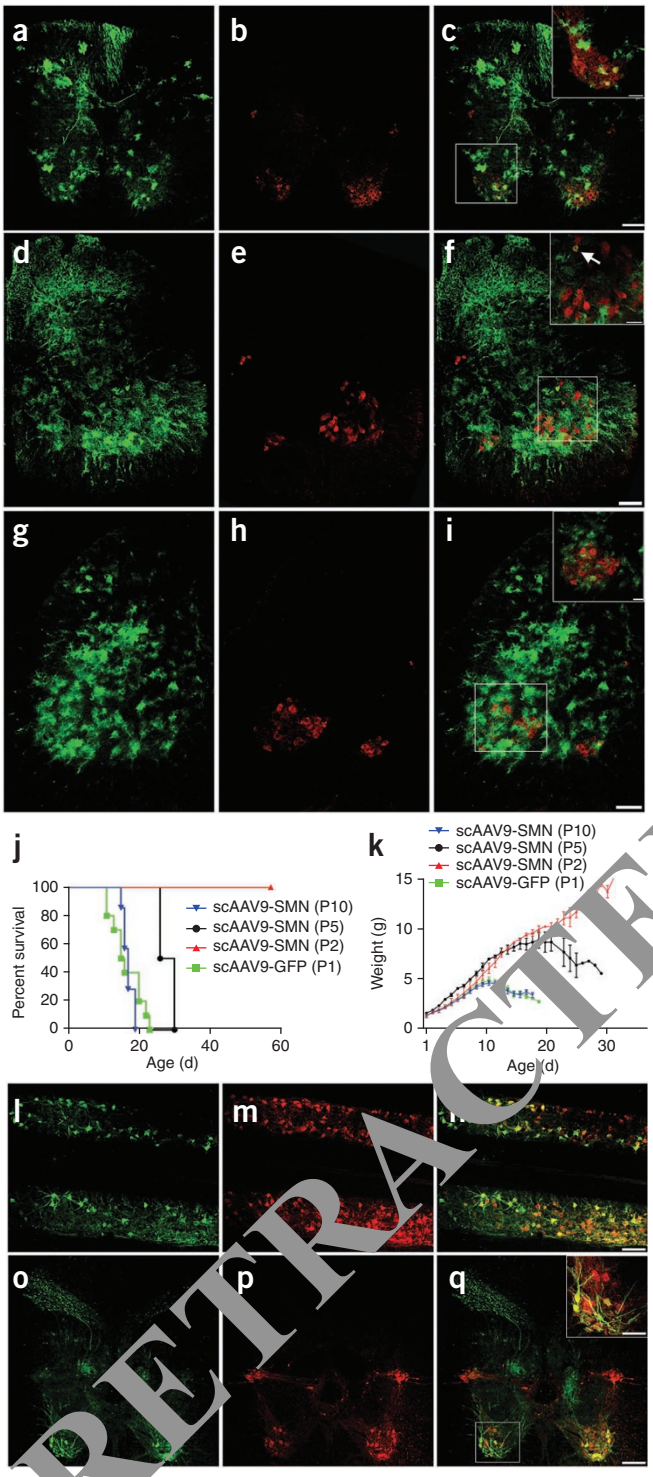

Figure 3 Systemic injection of scAAV9-GFP into SMA mice of varying ages. (**a**–**c**) Animals injected on P2 have a transduction pattern identical to P1-injected animals, with motoneuron transduction in lumbar spinal cord. (**d**–**f**) P5-injected animals have more glial transduction and less motoneuron (**f** inset, arrow) transduction than younger animals in lumbar spinal cord analysis. (**g**–**i**) The pattern of increasing glial transduction continues in P10-injected animals. GFP (green), ChAT (red, a motoneuron marker) and merged (yellow). (**j**–**k**) scAAV9-SMN injection on P2 in SMA animals rescues life span and increases body weight ($n = 6$), whereas P5 scAAV9-SMN delivery in SMA animals only partially rescues life span and body weight ($n = 4$) compared with control scAAV9-GFP–treated ($n = 10$). No increase in life span or body weight was seen in mice treated with scAAV9-SMN on P10 ($n = 4$). (**l**–**q**) Systemic injection of scAAV9-GFP into a cynomolgus macaque on P1 results in a similar transduction pattern within the spinal cord as previously shown in P1-injected mice. GFP (**l**,**m**), ChAT (**n**,**p**) and merged (**n**,**q**) images from thoracic spinal cord demonstrate motor neuron transduction. A representative longitudinal section is shown in (**l**–**n**), indicating transduction along the neuraxis. Transverse sections (**o**–**q**) mimic the pattern of dorsal root ganglia and motor neuron transduction seen in P1-injected mice. Inset scale bars, 50 μm; **c**,**f**,**i**, 100 μm; **n**,**q**, 200 μm.

slightly reduced (control = 61.3 ± 3.5; SMA-treated = 50.3 ± 2.6, $P < 0.05$) but was compensated for by a statistically significant increase in quantal amplitude (**Fig. 2b**; control = 1.39 ± 0.06; SMA-treated = 1.74 ± 0.08, $P < 0.05$). Quantal amplitudes in young animals had no significant differences (control = 1.6 ± 0.1, untreated SMA = 1.3 ± 0.1, treated SMA = 1.1 ± 0.1 nA, $P = 0.28$).

The reduction in vesicle release in untreated SMA mice was due to a decrease in probability of vesicle release, demonstrated by increased facilitation of EPCs during repetitive stimulation[15]. Both control and treated SMA EPCs were reduced by close to 20% by the 10th pulse of a 50 Hz train of stimuli (**Fig. 2c**, 22 ± 3% reduction in control versus 19 ± 1% reduction in treated SMA, $P = 0.36$). This suggests that the reduction in probability of release was corrected by replacement of SMN. During electrophysiologic recording, no evidence of denervation was noted. Furthermore, all adult NMJs analyzed showed normal morphology and full maturity (**Fig. 2d–i**). P9–P10 transverse abdominis immunohistochemistry showed the typical neurofilament accumulation in untreated SMA NMJs[15,17–19], whereas treated SMA NMJs showed a marked reduction in neurofilament accumulation (**Supplementary Fig. 5**).

A recent study using a histone deacetylase inhibitor to extend survival of SMA mice reported necrosis of the extremities and internal tissues[20]. In our study, mice developed necrotic pinna between P45–P70 (**Supplementary Fig. 6**). Pathological examination of the pinna revealed vascular necrosis, but necrosis was not found elsewhere. We previously demonstrated that vascular endothelium was among the cell types transduced after systemic scAAV9 delivery[2]. Lack of necrosis in the tail and hind-paws could be due to treatment of vascular tissue, whereas the development of the pinna after P1 precludes correction of this tissue owing to loss of recombinant vector genomes in dividing cells[21–23].

To explore the therapeutic window in SMA mice, we performed systemic scAAV9-GFP injections at varying postnatal time points to evaluate the pattern of transduction of motor neurons and astrocytes. scAAV9-GFP systemic injections in mice on P2, P5 or P10 showed distinct differences in the spinal cord. There was a shift from neuronal transduction in P2-treated animals toward predominantly glial transduction in older, P10 animals, consistent with our previous studies and knowledge of the developing blood-brain barrier in mice (**Fig. 3a–i**)[2,24].

To determine the therapeutic effect of SMN delivery at these various time points, small cohorts of SMA-affected mice were injected with scAAV9-SMN on P2, P5 and P10 and evaluated for changes in survival and body weight (**Fig. 3j–k**). P2-injected animals were rescued and indistinguishable from animals injected with scAAV9-SMN on P1. However, P5-injected animals showed a more modest increase in survival of ~15 d, whereas P10-injected animals were indistinguishable from GFP-injected SMA pups. These findings support previous studies demonstrating the importance of increasing SMN levels in neurons of SMA mice[8]. Furthermore, these results suggest a finite period during development in which intravenous injection of scAAV9 can target neurons in sufficient numbers for benefit in SMA.

To assess the potential for clinical translation of this approach, we investigated whether scAAV9 can traverse the blood–brain barrier in nonhuman primates[25]. We intravenously injected a male cynomolgus macaque on P1 with 1×10^{14} particles (2.2×10^{11} particles/g of body weight) of scAAV9-GFP and euthanized it 25 d after injection. Examination of the spinal cord revealed robust GFP expression within the dorsal root ganglia and motor neurons along the entire neuraxis (**Fig. 3l–q**), as seen in P1-injected mice. This finding demonstrates that early systemic delivery of scAAV9 can efficiently target motor neurons in a nonhuman primate.

In conclusion, we report here the most robust postnatal rescue of SMA mice to date, with correction of motor function, neuromuscular electrophysiology and survival after a one-time delivery of *SMN*. Intravenous scAAV9 treats neurons, muscle and vascular endothelium, all of which have been proposed as target cells for treatment[2]. Although this study did not attempt to dissect the roles of different cell types in SMA, our P10 data show that SMN replacement in astrocytes is not effective in delaying disease, consistent with previous results using transgenic approaches[8]. We have also defined a window of opportunity for targeting motor neurons in neonates. Future studies in nonhuman primates will further elucidate a therapeutic window more relevant to human therapy. Advances in vector design, such as AAV capsid modification, mutagenesis or gene shuffling, may expand the opportunity to target neurons in the adult[26–28]. Although SMA children are often asymptomatic at birth, newborn screening that can detect SMA has been developed, supporting the feasibility of delivering scAAV9-SMN to affected children[29]. Additionally, we have demonstrated widespread transduction within the spinal cord of a nonhuman primate species. We are continuing to advance this delivery system in nonhuman primates and evaluating immunological consequences to the SMN gene and AAV capsid in order to set the stage for human clinical trials of scAAV9-SMN in SMA. Given that SMA is a disease of low versus no protein, we do not anticipate an immune response against the *SMN* transgene. Further, we expect gene delivery to newborn patients to occur prior to wild-type AAV infection, thereby lowering the chances of preexisting immunity to the AAV capsid.

METHODS

Methods and any associated references are available in the online version of the paper at http://www.nature.com/nature/technology/.

Note: Supplementary information is available on the Nature Biotechnology website.

ACKNOWLEDGMENTS
This work was supported by NIH/NINDS P21NS064328 to B.K.K., NINDS R01NS038650 to A.H.M.B., NINDS core P30-NS045758, RC2 NS069476-01 and Miracles for Madison Fund to B.K.K. and A.H.M.B. and NINDS P01NS057228 to M.M.R. We thank K. Levine and E. Nurre for expert technical assistance and J. Ward for pathology services.

AUTHOR CONTRIBUTIONS
K.D.F., M.M.R., A.H.M.B. and B.K.K. designed and executed experiments and wrote the manuscript. V.L.M., X.W, L.B., A.M.H., A.K.B., P.R.M. and T.T.L. contributed to experiments.

COMPETING INTERESTS STATEMENT
The authors declare no competing financial interests.

Published online at http://www.nature.com/naturebiotechnology/.
Reprints and permissions information is available online at http://npg.nature.com/reprintsandpermissions/.

1. Burghes, A.H. & Beattie, C.E. Spinal muscular atrophy: why do low levels of survival motor neuron protein make motor neurons sick? *Nat. Rev. Neurosci.* **10**, 597–609 (2009).
2. Foust, K.D. *et al.* Intravascular AAV9 preferentially targets neonatal neurons and adult astrocytes. *Nat. Biotechnol.* **27**, 59–65 (2009).
3. Gao, G. *et al.* Clades of adeno-associated viruses are widely disseminated in human tissues. *J. Virol.* **78**, 6381–6388 (2004).
4. McCarty, D.M. *et al.* Adeno-associated virus terminal repeat (TR) mutant generates self-complementary vectors to overcome the rate-limiting step to transduction *in vivo*. *Gene Ther.* **10**, 2112–2118 (2003).
5. Lefebvre, S. *et al.* Identification and characterization of a spinal muscular atrophy-determining gene. *Cell* **80**, 155–165 (1995).
6. McGovern, V.L., Gavrilina, T.O., Beattie, C.E. & Burghes, A.H. Embryonic motor axon development in the severe SMA mouse. *Hum. Mol. Genet.* **17**, 2500–2509 (2008).
7. MacKenzie, A.E. & Gendron, N.H. Tudor reign. *Nat. Struct. Biol.* **8**, 13–15 (2001).
8. Gavrilina, T.O. *et al.* Neuronal SMN expression corrects spinal muscular atrophy in severe SMA mice while muscle-specific SMN expression has no phenotypic effect. *Hum. Mol. Genet.* **17**, 1063–1075 (2008).
9. Azzouz, M. *et al.* Lentivector-mediated SMN replacement in a mouse model of spinal muscular atrophy. *J. Clin. Invest.* **114**, 1726–1731 (2004).
10. Avila, A.M. *et al.* Trichostatin A increases SMN expression and survival in a mouse model of spinal muscular atrophy. *J. Clin. Invest.* **117**, 659–671 (2007).
11. Hastings, M.L. *et al.* Tetracyclines that promote SMN2 exon 7 splicing as therapeutics for spinal muscular atrophy. *Sci. Transl. Med* **1**, 5–14 (2009).
12. Duque, S. *et al.* Intravenous administration of self-complementary AAV9 enables transgene delivery to adult motor neurons. *Mol. Ther.* **17**, 1187–1196 (2009).
13. Le, T.T. *et al.* SMNDelta7, the major product of the centromeric survival motor neuron (SMN2) gene, extends survival in mice with spinal muscular atrophy and associates with full-length SMN. *Hum. Mol. Genet.* **14**, 845–857 (2005).
14. Butchbach, M.E.R., Edwards, J.D. & Burghes, A.H. Abnormal motor phenotype in the SMNDelta7 mouse model of spinal muscular atrophy. *Neurobiol. Dis.* **27**, 207–219 (2007).
15. Kong, L. *et al.* Impaired synaptic vesicle release and immaturity of neuromuscular junctions in spinal muscular atrophy mice. *J. Neurosci.* **29**, 842–851 (2009).
16. Wang, X. *et al.* Decreased synaptic activity shifts the calcium dependence of release at the mammalian neuromuscular junction in vivo. *J. Neurosci.* **24**, 10687–10692 (2004).
17. Fuentes-Diaz, C. *et al.* Neurofilament accumulation at the motor endplate and lack of axonal sprouting in a spinal muscular atrophy mouse model. *Hum. Mol. Genet.* **11**, 1439–1447 (2002).
18. Kariya, S. *et al.* Reduced SMN protein impairs maturation of the neuromuscular junctions in mouse models of spinal muscular atrophy. *Hum. Mol. Genet.* **17**, 2552–2569 (2008).
19. Murray, L.M. *et al.* Selective vulnerability of motor neurons and dissociation of pre- and post-synaptic pathology at the neuromuscular junction in mouse models of spinal muscular atrophy. *Hum. Mol. Genet.* **17**, 949–962 (2008).
20. Narver, H.L. *et al.* Sustained improvement of spinal muscular atrophy mice treated with trichostatin A plus nutrition. *Ann. Neurol.* **64**, 465–470 (2008).
21. Clark, K.R. *et al.* Gene transfer into the CNS using recombinant adeno-associated virus: analysis of vector DNA forms resulting in sustained expression. *J. Drug Target.* **7**, 269–283 (1999).
22. Duan, D. *et al.* Circular intermediates of recombinant adeno-associated virus have defined structural characteristics responsible for long-term episomal persistence in muscle tissue. *J. Virol.* **72**, 8568–8577 (1998).
23. Nakai, H. *et al.* Extrachromosomal recombinant adeno-associated virus vector genomes are primarily responsible for stable liver transduction in vivo. *J. Virol.* **75**, 6969–6976 (2001).
24. Saunders, N.R., Joakim Ek, C. & Dziegielewska, K.M. The neonatal blood-brain barrier is functionally effective, and immaturity does not explain differential targeting of AAV9. *Nat. Biotechnol.* **27**, 804–805, author reply 805 (2009).
25. Kota, J. *et al.* Follistatin gene delivery enhances muscle growth and strength in nonhuman primates. *Sci. Transl. Med* **1**, 6–15 (2009).
26. Koerber, J.T. *et al.* Molecular evolution of adeno-associated virus for enhanced glial gene delivery. *Mol. Ther.* **17**, 2088–2095 (2009).
27. Maheshri, N., Koerber, J.T., Kaspar, B.K. & Schaffer, D.V. Directed evolution of adeno-associated virus yields enhanced gene delivery vectors. *Nat. Biotechnol.* **24**, 198–204 (2006).
28. Asokan, A. *et al.* Reengineering a receptor footprint of adeno-associated virus enables selective and systemic gene transfer to muscle. *Nat. Biotechnol.* **28**, 79–82 (2010).
29. Pyatt, R.E., Mihal, D.C. & Prior, T.W. Assessment of liquid microbead arrays for the screening of newborns for spinal muscular atrophy. *Clin. Chem.* **53**, 1879–1885 (2007).

ONLINE METHODS

Review board approval. All animal procedures were approved by Nationwide Children's Hospital Institutional Animal Care and Use Committee, Wright State Institutional Animal Care and Use Committee, The Mannheimer Foundation Animal Care and Use Committee and Ohio State University Animal Care and Use Committee.

Animals. SMA parent mice (*Smn*$^{+/-}$, *SMN2*$^{+/+}$, SMNΔ7$^{+/+}$) were time mated[30]. Cages were monitored 18–21 d after visualization of a vaginal plug for the presence of litters. Once litters were delivered, the mother was separated from pups, pups were given tattoos for identification and tail samples were collected. Tail samples were incubated in lysis solution (25 mM NaOH, 0.2 mM EDTA) at 90 °C for 1 h. After incubation, tubes were placed on ice for 10 min then received an equal volume of neutralization solution (40 mM Tris pH5). After the neutralization buffer, the extracted genomic DNA was added to two different PCR reactions for the mouse *Smn* allele (Forward 1: 5′-TCCAGCTC CGGGATATTGGGATTG, Reverse 1: 5′-AGGTCCCACCACCTAAGAAAGCC, Forward 2: 5′-GTGTCTGGGCTGTAGGCATTGC, Reverse 2: 5′-GCTG TGCCTTTTGGCTTATCTG) and one reaction for the mouse *Smn* knockout allele (Forward: 5′-GCCTGCGATGTCGGTTTCTGTGAGG, Reverse: 5′-CCAGCGCGGATCGGTCAGACG). After analysis of the genotyping PCR, litters were culled to three animals. Affected animals (*Smn*$^{-/-}$, *SMN2*$^{+/+}$, *SMNΔ7*$^{+/+}$) were injected as previously described with 5×10^{11} particles of scAAV9-SMN or scAAV9-GFP[2].

Ultrasound-guided intracardiac delivery of scAAV9. In older mice we used ultrasound-guided intracardiac injections to efficiently deliver the gene therapy vector. Animals were anesthetized using 1–2.5% isofluorane (in O_2 gas) throughout the procedure. Animals were secured with tape to a heated platform and fitted with a nose cone. A Vevo 2100 ultrasound was used to visualize the animal's heart and monitor vitals. For scAAV9-GFP injections into wild-type mice, P5 animals were injected with 7E+11 vector genomes (vg, in 70 µl), P10 animals with 3.5E+11vg (in 70 µl), into the left ventricle. Affected mice were similarly injected with scAAV9-SMN on P5 and P10 with 3E+11vg (in 60 µl). Upon successful vector delivery, the animals were monitored for signs of cardio-pulmonary distress, disconnected from the anesthetic machine and placed in an oxygen recovery chamber for a short period of time before being returned to its cage.

Nonhuman primate subjects. The selected experimental subject was a 1-d-old cynomolgus macaque (*Macaca fascicularis*) born in December 2009, at The Mannheimer Foundation, an Association for Assessment and Accreditation of Laboratory Animal Care International-accredited facility. The dam and sire of this neonate were both part of the cynomolgus breeding colony at the Foundation, housed in an outdoor enclosure. All cynomolgus macaques at the Foundation are fed a commercial diet (Harlan Teklad 2050), supplemented with seeds, fruits/produce and primate biscuits, fresh water *ad libitum*. All uses and procedures were approved and in accordance with the Institutional Animal Care and Use Committee (IACUC) of the Mannheimer Foundation. Both dam and newborn were negative for selected retroviruses (simian immunodeficiency virus, simian retrovirus type D and simian T-cell lymphotropic virus type 1) and B virus (cercopithecine herpes virus 1).

AAV9 administration to nonhuman primates. As soon as the newborn subject was identified and selected in the outdoor enclosure, it was brought into an indoor isolation room on the same birth-day and pair-housed along with its dam. Within 24 h of the birth and just before the AAV9 delivery both dam and newborn were sedated with ketamine HCL (at a dose of 10 mg/kg intramuscular) and briefly separated from each other to perform the initial procedures. Baseline blood samples were collected from both dam and newborn through femoral venipunctures. After blood samples were collected, the dam was placed back in its cage; the newborn was positioned on sternal recumbency, and one of its legs shaved/disinfected in preparation for the intravenous injection of the AAV9. A 24-gauge intravenous catheter was placed into the saphenous vein. Vector solution was drawn into a 12 cc syringe pre-wetted with saline solution (0.9% NaCl). The intravenous catheter was flushed and its patency verified by using ~1 cc of the same saline solution. A total volume of 10 cc of the AAV9 was delivered intravenously (medium dose of 1-5E+12 vg/g) in a bolus fashion. After injection, the newborn was recovered in a controlled temperature isolette (set at 95 °F) and returned to its dam after full recovery was achieved.

Perfusion-fixation procedures and organ collections. 25 d post-AAV9 injection dam and infant were accessed once more by sedation with ketamine HCL (at a dose of 10 mg/kg) and Telazol (at a dose of 5 mg/kg), respectively. A follow-up blood sample was collected from the dam; the infant was separated and taken to the necropsy room for its terminal collections and procedures. A 24-gauge intravenous catheter was placed into a saphenous vein to facilitate subsequent doses of the anesthetic drug and the delivery of the euthanasia solution. Once the infant was confirmed to be in a deep anesthetic plane, a blood sample was collected, and then both thoracic and abdominal cavities were exposed to proceed with the perfusion process. A 20-gauge needle was inserted intra-cardially into the left ventricle, the right auricle was sectioned and the perfusion started first with 0.9% NaCl and then with 4% paraformaldehyde solution. A total of ~1.5 liters of the solution were perfused by gravity flow. Upon completion of the perfusion, several sections of major organs were harvested and fixed by immersion using the same paraformaldehyde solution.

Viral vector. AAV9 was produced by transient transfection procedures using a double-stranded AAV2 ITR–based vector-GFP vector, with a plasmid encoding Rep2Cap9 sequences as previously described[3] along with a adenoviral helper plasmid; pHelper (Stratagene) in HEK293 cells. Our serotype 9 sequence was verified by sequencing and identical to that previously described[3]. Virus was purified by two cesium chloride density gradient purification steps, dialyzed against PBS and formulated with 0.001% Pluronic-F68 to prevent virus aggregation and stored at 4 °C. All vector preparations were titered by quantitative-PCR using TaqMan technology. Purity of vectors was assessed by 4–12% SDS polyacrylamide gel electrophoresis and silver staining (Invitrogen).

Behavior. Pups were weighed daily and tested for righting reflex every other day from P5–P13. Pups were placed on their sides and time to right was recorded, with a maximum of 30 sec allowed[14]. Every 5 d between P15 and P30, animals were tested in an open field analysis (San Diego Instruments). Animals were given several minutes within the testing chamber before the beginning of testing, then activity was monitored for 5 min. Beam breaks were recorded in the x, y and z planes, averaged across groups at each time point, then graphed.

Immunofluorescence. Whole mount tissue. Whole mount TVA muscle was blocked in 10% Tween-20 (Sigma), 4% goat serum (Sigma) and PBS for 30 min. Whole mount tissue was incubated with goat anti-mouse neurofilament 160, (1:500, Chemicon) in 10% Tween-20, 0.4% goat serum, PBS overnight and incubated with Alexa Fluor-488 anti-mouse secondary antibody (1:1,000, Molecular Probes) for 2 h, and Alexa Fluor594 alpha-bungarotoxin (1:1,000, Molecular Probes) for 30 min. Tissues were mounted in Vectashield (Vector Labs).

Tissue sections. Whole mount TVA muscle were post-fixed in 4% paraformaldehyde then stained with chicken anti-mouse neurofilament heavy chain, (1:1000, EnCor Biotechnology) in 10% Tween-20, 0.4% goat serum, PBS for 2 h and incubated with Alexa Fluor 488 anti-chicken secondary antibody (1:1000, Molecular Probes) and AlexaFluor594 alpha-bungarotoxin (1:1,000) for 30 min. Tissue sections were mounted in Vectashield.

Confocal microscopy. All images were captured with the Leica TCS_SL scanning confocal microscope system using an inverted Leica DMIRE2 microscope and PMT detectors. Images were captured at 25°C with the following objective: 63× HCX Plan Apo CS oil, NA = 1.4.0. A Z-Galvo stage was used to obtain z-series stacks of ~30 images each. Image acquisition, overlays, scale bars and measurements were produced with the Leica Confocal Software v2.61, and subsequent image processing was performed with Adobe Photoshop CS2.

Cell counts. For both GFP and Gem quantifications, spinal cords from fixed animals were removed from the carcass. Lumbar enlargements were blocked

and sliced into 40-μm thick sections on a vibratome (Leica). Sections were collected in order in a 96-well plate. Every 12th section was sampled for a total of eight sections spanning ~3.8 mm. The sections were fluorescently labeled using immunohistochemistry against choline acetyl transferase, green fluorescent protein or survival motor neuron. Sections were counted using the 63× objective on a confocal microscope. Greater detail on the extent of central nervous system transduction by scAAV9 following P1 injection is shown in previous work[30].

Western blot analysis. 100 mg of tissue was homogenized in Tissue Protein Extraction Reagent (Pierce). The sample was mixed with an equal volume of loading buffer (62.5 mM Tris, pH 6.8, 20% glycerol, 200 mM DTT, 0.2% bromophenol blue) and run on a 12.5% polyacrylamide gel. Samples were transferred to Immobilon-P (Millipore). The blot was blocked in 5% milk powder, 0.5% BSA in PBS-Tween for 1 h, and then incubated for 1 h with a primary antibody cocktail of MANSMA 2, 7, 13 and 19. Bound primary antibody was detected by horseradish peroxidase conjugated secondary antibody followed by chemiluminescence (ECL Western Blotting Detection Reagents, Amersham Biosciences). The blots were then stripped and reprobed with a β-actin monoclonal antibody (clone AC-15, Sigma-Aldrich) or a GAPDH monoclonal antibody (Millipore) to control for protein loading.

Electrophysiology. The recording chamber was continuously perfused with Ringer's solution containing the following (in mmol/l): 118 NaCl, 3.5 KCl, 2 $CaCl_2$, 0.7 $MgSO_4$, 26.2 $NaHCO_3$, 1.7 NaH_2PO_4 and 5.5 glucose, pH 7.3–7.4 (20–22 °C, equilibrated with 95% O_2 and 5% CO_2). Endplate recordings were performed as follows. After dissection, the tibialis anterior muscle was partially bisected and folded apart to flatten the muscle. After pinning, muscle strips were stained with 10 μM 4-Di-2ASP [4-(4-diethylaminostyryl)-*N*-methylpyridinium iodide] (Molecular Probes) and imaged with an upright epifluorescence microscope. At this concentration, 4-Di-2ASP staining enabled visualization of surface nerve terminals as well as individual surface muscle fibers. All of the endplates were imaged and impaled within 100 μm. We used two-electrode voltage clamp to measure endplate current (EPC) and miniature EPC (MEPC) amplitude. Muscle fibers were crushed away from the endplate band and voltage clamped to −45 mV to avoid movement after nerve stimulation.

Statistics. Statistical analyses were performed using GraphPad Prism software. Means were represented with s.e.m. Student *t*-tests were performed to compare groups using a 95% confidence level. Kaplan Meier Survival analysis was performed.

30. Monani, U.R. *et al.* The human centromeric survival motor neuron gene (*SMN2*) rescues embryonic lethality in *Smn*−/− mice and results in a mouse with spinal muscular atrophy. *Hum. Mol. Genet.* 333–339 (2000).

doi:10.1038/nbt.1610